

GA-A27324

# FUELING WITH EDGE RECYCLING TO HIGH DENSITY IN DIII-D

By

A.W. LEONARD, J.D. ELDER, J.M. CANIK, R.J. GROEBNER, and  
T.H. OSBORNE

JULY 2012



## DISCLAIMER

**This report was prepared as an account of work sponsored by an agency of the United States Government. Neither the United States Government nor any agency thereof, nor any of their employees, makes any warranty, express or implied, or assumes any legal liability or responsibility for the accuracy, completeness, or usefulness of any information, apparatus, product, or process disclosed, or represents that its use would not infringe privately owned rights. Reference herein to any specific commercial product, process, or service by trade name, trademark, manufacturer, or otherwise, does not necessarily constitute or imply its endorsement, recommendation, or favoring by the United States Government or any agency thereof. The views and opinions of authors expressed herein do not necessarily state or reflect those of the United States Government or any agency thereof.**

GA-A27324

# FUELING WITH EDGE RECYCLING TO HIGH DENSITY IN DIII-D

By

A.W. LEONARD<sup>1</sup>, J.D. ELDER<sup>2</sup>, J.M. CANIK<sup>3</sup>, R.J. GROEBNER<sup>1</sup>, and  
T.H. OSBORNE<sup>1</sup>

This is a preprint of a paper to be presented at the Twentieth International Conference on Plasma-Surface Interactions in Controlled Fusion Devices, May 21–25, 2012 in Aachen, Germany and to be published in the *J. Nucl. Mater.*

<sup>1</sup>General Atomics, P.O. Box 85608, San Diego, California, USA

<sup>2</sup>University of Toronto Institute of Aerospace Studies, Toronto, Canada

<sup>3</sup>Oak Ridge National Laboratory, P.O. Box 2008, Oak Ridge, Tennessee, USA

Work supported in part by  
the U.S. Department of Energy  
under DE-FC02-04ER54698, AND DE-AC05-00OR22725

GENERAL ATOMICS PROJECT 30200  
JULY 2012



## FUELING WITH EDGE RECYCLING TO HIGH-DENSITY IN DIII-D

A.W. Leonard<sup>a\*</sup>, J.D. Elder<sup>b</sup>, J.M. Canik<sup>c</sup>, R.J. Groebner<sup>a</sup>, and T.H. Osborne<sup>a</sup>

<sup>a</sup>*General Atomics, P.O. Box 85608, San Diego, CA 92186-5608, USA*

<sup>b</sup>*University of Toronto Institute of Aerospace Studies, Toronto, M3H 5T6, Canada*

<sup>c</sup>*Oak Ridge National Laboratory, P.O. Box 2008, Oak Ridge, TN 37831, USA*

**Abstract.** Pedestal fueling through edge recycling is examined with the interpretive OEDGE code for high-density discharges in DIII-D. A high current, high-density discharge is found to have a similar ionization source profile as a lower current, lower density discharge. The higher density discharge, however, has a greater density gradient indicating a pedestal particle diffusion coefficient that scales near linear with  $1/I_p$ . The time dependence of density profile is taken into account in the analysis of a discharge with low frequency ELMs. The time-dependent analysis indicates that the inferred neutral ionization source is inadequate to account for the increase in the density profile between ELMs, implying an inward density convection, or density pinch, near the top of the pedestal.

### 1. Introduction

A significant concern for next step burning plasma tokamaks is the achievement of the high density required for high fusion gain. It is envisioned that strong central fueling, such as pellet injection, will be required to achieve this density since recycled neutrals will not penetrate significantly beyond the separatrix in larger scale tokamaks. [1,2] While some experimental studies [3] have found a correlation between the neutral ionization profile and the pedestal density profile, other results [4,5] and theoretical considerations [6] suggest that non-diffusive processes, such as a particle pinch, may lead to a higher density in the edge pedestal than would be expected from neutral recycling alone. This study examines the neutral ionization rate within the pedestal and core of high-density discharges in DIII-D with the goal of determining whether an inward plasma convection, or pinch, is required to achieve the observed density profiles.

The establishment of the pedestal density profile can be examined with the particle diffusion equation,  $D\partial n/\partial r = -\Gamma + nv_r$ , where  $D$  is the diffusion coefficient,  $\Gamma$  is the radial ion flux, and  $v_r$  is a potential radial convective velocity. Typical analysis of pedestal transport assumes  $v_r$  to be zero because the relative strength of the diffusive and convective terms cannot be readily assessed. However for regions of very low, or even inward, radial ion flux, a convective inward flux would be required to drive a significant density gradient in the pedestal, without an unphysical low, or even negative diffusion coefficient. The establishment of inward convection playing a role in setting the pedestal density profile would indicate the potential for achieving high core density in future tokamaks without the need for direct central fueling.

Two high-density discharges are examined in DIII-D with the potential to limit the penetration of recycling neutrals and thus reduce the radial ion flux within the steep density gradient region of the pedestal. The ionization and radial ion flux profiles

within the separatrix are examined with the interpretive modeling OEDGE code [7]. The first scenario is carried out at high current, 2.0 MA, with the toroidal field  $\nabla B$  drift direction away from the X-point to keep the inboard divertor at high electron temperature and limit the penetration of recycled neutrals. A comparison of a 2.0 MA to a 1.0 MA discharge reveals nearly a doubling of the pedestal density while the inferred radial ion flux does not change significantly

The second scenario examined in this study is a 1.5 MA discharge with standard toroidal field direction, but at lower power with infrequent ELMs. Time-dependent analysis finds the core density increase inside the top of the pedestal between ELMs is greater than can be accounted for by the edge recycling and neutral beam heating ionization sources. This analysis indicates a density pinch is required to account for the density profile evolution inward of the top of the pedestal.

In section 2 the steady state case experimental details and modeling of pedestal fueling are presented. The time dependent case experimental setup and modeling are presented in section 3. In section 4 the implications of the density and ionization profiles for a particle pinch are discussed.

## 2. Constant pedestal conditions

The first case examined is a Lower-Single-Null (LSN) configuration with moderate triangularity,  $\langle \delta \rangle = 0.35$ , where a high plasma current discharge, 2.0 MA, is compared to a lower current, 1.0 MA discharge. The 2.0 MA discharge was run with a toroidal field of 2.1 T with  $q_{95} \sim 2.6$ . The toroidal field was run with the  $\nabla B$  drift direction out of the divertor in order to avoid detachment of the inboard divertor plasma and limit penetration of the recycling neutrals. H-mode was obtained with an input power of 7.8 MW of neutral beam injection (NBI). A line-averaged density of  $1.2 \times 10^{20} \text{ m}^{-3}$  was achieved during H-mode with no external gas puffing. For a comparison, a plasma with greater neutral penetration was run at 1.0 MA with  $B_t = 1.05 \text{ T}$  and the same shape and  $q_{95}$ . An NBI power of 2.6 MW obtained H-mode with a density of  $6.5 \times 10^{19} \text{ m}^{-3}$ , also without external gas puffing. Both cases had regular large Type I ELMs at 25 Hz, or a period of  $\sim 40 \text{ ms}$  between ELMs.

The pedestal and SOL profiles of  $n_e$  and  $T_e$  for these discharges were analyzed using Thomson Scattering, with data collected in the last 20% of the ELM cycle, over a 1 second period of nearly stationary ELM conditions. The  $n_e$  and  $T_e$  profiles shown in Fig. 1 indicate a 2.0 MA discharge pedestal density of nearly  $1.0 \times 10^{20} \text{ m}^{-3}$ ,  $\sim 70\%$  greater than the 1.0 MA pedestal at  $6.0 \times 10^{19} \text{ m}^{-3}$ . The density pedestal width was somewhat narrower at high current. The pedestal temperature is also about double at 2.0 MA compared to 1.0 MA resulting in an electron

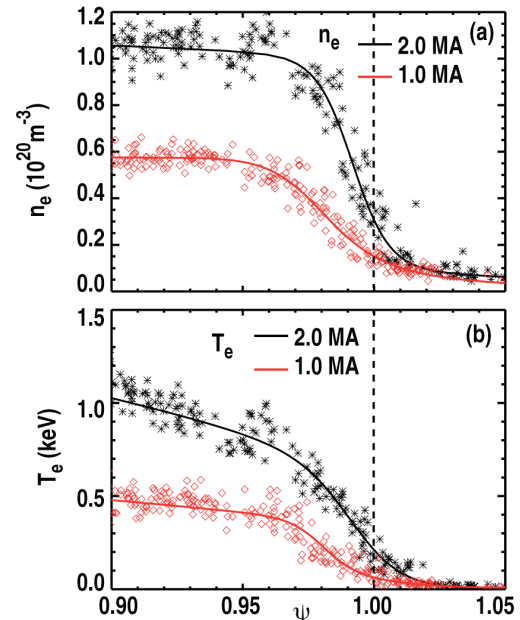


Fig. 1. The (a) electron density and (b) electron temperature in the pedestal and SOL from Thomson scattering extracted from the last 20% of the ELM cycle for the 1.0 MA and 2.0 MA discharges. The solid lines are tanh function fits to the data.

pressure approximately 4 times higher, for a constant pedestal  $\beta$ . Pedestal collisionality, however was somewhat reduced at higher current.

The 2D ionization profiles of these discharges are assessed by interpretive modeling with the OEDGE code [7]. This assessment begins with reconstruction of the SOL, divertor and pedestal plasma using all available diagnostics to constrain the modeled profiles as described in Ref. [8]. Neutrals are modeled with the EIRENE Monte Carlo code [9] where they are launched from all plasma facing surfaces with the same profile as the surface ion flux and followed until ionization. In addition a recombination source, consistent with the plasma reconstruction, is also included. In these analysis the recombination source was negligible. An important aspect of this analysis is to reconstruct the surface ion flux, and thus the neutral profile assuming unity recycling, as accurately as possible, and consistent with the background plasma reconstruction. The divertor ion flux and electron temperature profile is measured with target plate Langmuir probes, corroborated with IR camera measurements. The far SOL conditions were measured with an insertable Langmuir probe at the midplane to measure the decay length of  $n_e$  and  $T_e$ . This characteristic length was then used to project the plasma conditions, and particularly the ion flux, to all plasma facing surfaces in the vessel. Inside the separatrix the  $n_e$  and  $T_e$  profiles were fit to the Thomson Scattering measurements. This analysis is similar in approach to a previous DIII-D study utilizing the UEDGE fluid code [10], but the interpretive OEDGE code provides greater flexibility for matching multiple diagnostics and carrying out sensitivity studies.

The flux surface averaged ionization profiles for 2.0 MA and 1.0 MA discharges, modeled with OEDGE using the process described above are shown in Fig. 2. The modeled SOL density is higher than the measured density near the separatrix. This maybe due to an offset in the assumed separatrix location on the Thomson profile. This is not expected to significantly affect the ionization modeling, but future work will examine this sensitivity.

The ionization profiles of Fig. 2 are the result of recycled ion flux to all surfaces. However without external gas puffing the divertor source dominates the ionization source. Between ELMs the midplane limiter density is quite low,  $n_e \leq 1 \times 10^{18} \text{ m}^{-3}$ . The total wall ion flux, or total ionization assuming unity recycling, is  $1.1 \times 10^{23} \text{ s}^{-1}$  for the 2.0 MA discharge and  $0.4 \times 10^{23} \text{ s}^{-1}$  for 1.0 MA. Only about 5% of this flux is ionized inside the separatrix, or  $5.8 \times 10^{21} \text{ s}^{-1}$  at 2.0 MA and 17%, or  $7.0 \times 10^{21} \text{ s}^{-1}$  at 1.0 MA. Less than 10% of the core ionization is due to recycled ions from the main chamber. While the higher divertor density at high current results in a factor of 3 higher total neutral source, a larger fraction of that flux is ionized in the divertor outside the separatrix. This results in a small decrease in ionization within the pedestal at high current.

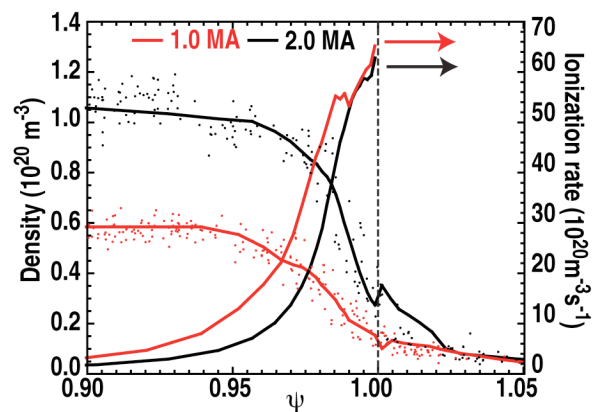


Fig. 2. The OEDGE modeled fit to the density profile for 2.0 MA and 1.0 MA. Also shown are the modeled flux surface averaged ionization profiles for 2.0 MA and 1.0 MA.

The radial ion flux can be inferred from ion conservation by assuming insignificant time-dependence and integrating the ionization source inside each flux surface as shown in Fig. 3. The neutral heating beam ionization source, a small contribution mostly at a radius inside of the pedestal, is included in this total at  $6.6 \times 10^{20}$  s<sup>-1</sup> at 2.0 MA and  $2.1 \times 10^{20}$  s<sup>-1</sup> at 1.0 MA. The most striking aspect of the radial ion flux in Fig. 3 is that the profile is very similar for both the high and low current cases. However, the 2.0 MA case is able to achieve a pedestal density  $\sim 75\%$  higher than at low current. If particle transport through the pedestal is diffusive, this would indicate a diffusion coefficient scaling roughly linear with  $1/I_p$ . This in itself does not confirm, or rule out, the presence of an inward particle pinch within the pedestal, but places an upper limit on particle transport coefficients. The implications of these trends will be discussed in Section 4.

### 3. Time-dependent analysis

The other case examined is a LSN discharge with plasma current of 1.5 MA and  $B_t$  of 2.1T for  $q_{95}$  of 3.5. The  $\nabla B$  drift direction was into the divertor in order to achieve H-mode with low NBI power, 2.2 MW, and infrequent ELMs. The resulting regular ELM period of 250 ms allows for examination of the evolution of the pedestal and core density profile from one ELM to the next. Over 2 seconds of constant conditions Thomson scattering data was sorted into the following phases of the ELM cycle; 20-40%, 40-60%, 60-80% and 80-99%. As shown in Fig. 4, the density continues to rise with the density pedestal building inward. From the middle of the pedestal outward through the SOL, plasma conditions remain constant from about 20 ms after an ELM until the next ELM. The divertor conditions also remain constant as evidenced from divertor IR camera heat flux, Da emission, and Langmuir probes at the target plate.

The edge ionization profile for this case was analyzed for the profiles in the middle of the ELM cycle, the 40-60% profile, Fig. 5. As in the previous case, the SOL density and temperature profiles are modeled with the OEDGE code, with boundary conditions for the divertor target plate profiles from Langmuir probes and IR camera.

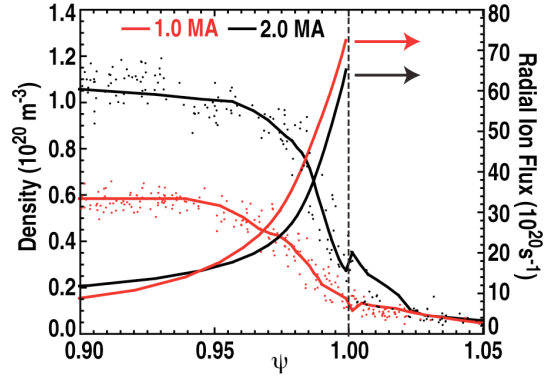


Fig. 3. The radial ion flux profiles inferred from the modeled ionization profiles for 2.0 MA and 1.0 MA.

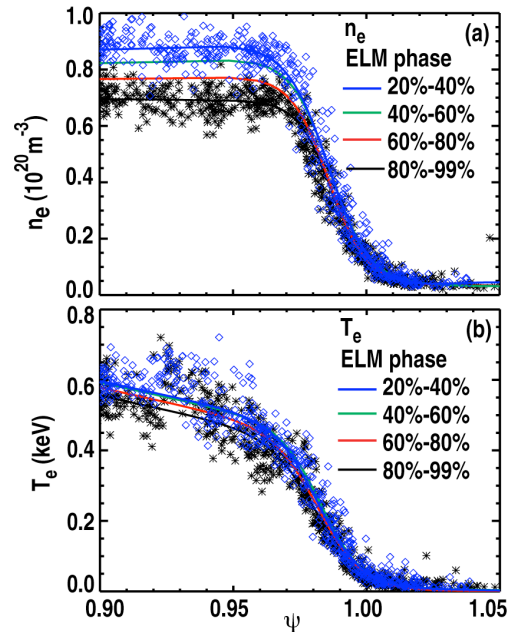


Fig. 4. The (a) electron density and (b) electron temperature profiles from Thomson scattering data sorted with respect to ELM phase. The solid lines are modified tanh function fits to the data.

The SOL  $n_e$  and  $T_e$  profiles were fit to an exponential function constrained by the upstream Thomson scattering measurements and midplane Langmuir probe data, similar to the previous case. One uncertainty in the reconstruction of SOL and divertor plasma for this case was coverage of the inner strike-point by the Langmuir probe array. To assess this uncertainty the model was run with two different inner divertor profiles spanning the uncertainty of a factor of 2 in ion flux to the inner divertor.

The resulting radial profile of flux-surface-averaged ionization is also shown in Fig. 5. This profile is similar to the previous case in that the ionization scale length is very similar to the pedestal density profile. The error bars in the figure represent the sensitivity of the ionization profile to a factor of two uncertainties in the inner divertor ion flux. The recycled neutrals from main chamber ion flux outside of the divertor represent about 1/3 of this ionization profile. Though this is a higher fraction than the previous steady state case this still indicates that the ionization profile is less dependent on main chamber ion flux uncertainties.

The role of the ionization profile in accounting for the density rise between ELMs can be examined in the context of particle continuity,  $\nabla \cdot \Gamma = S_0 - \partial n / \partial t$ . By integrating both the density increase and the ionization profile from the plasma center to a radius  $r$ , the radial profile of the ion flux can be determined from  $\Gamma = \int_0^r S_0 - \int_0^r \partial n / \partial t$ . The analysis of these two terms for the edge plasma, from  $\psi = 0.8$  to  $\psi = 1.0$  is shown in Fig. 6.

The  $dn_i / dt$  curve represents the increase in main ion density inside the flux surface  $\psi$ . Since the modeling represents deuterium ionization, dilution of the main ion density by carbon impurity is taken into account by charge exchange spectroscopy (CER) measurements, indicating the main ion deuterium density is roughly 80% of the electron density throughout the ELM cycle. The integrated ion density increase is relatively flat throughout the edge and pedestal region. This is consistent with the density profiles of Fig. 4, where the density profile from the top of the pedestal inward increases from one ELM to the next, while the density within the pedestal itself does not vary significantly.

The ionization sources plotted in Fig. 6 include both the edge recycling source and the neutral beam heating source. The recycling ionization source is the ionization profile of Fig. 5 integrated from the plasma center to the flux surface  $\psi$ . The beam ionization source is relatively small, but flat across the profile as most of the beam

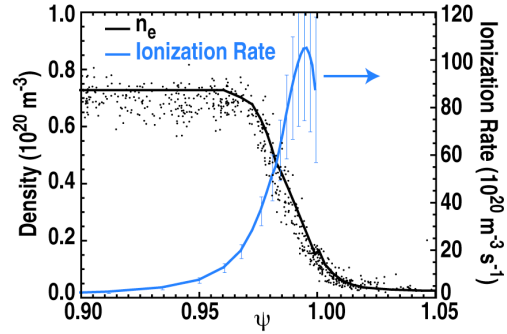


Fig. 5. The OEDGE modeled density profile for the 40%-60% ELM phase. Also shown is the OEDGE modeled flux surface averaged ionization profile.

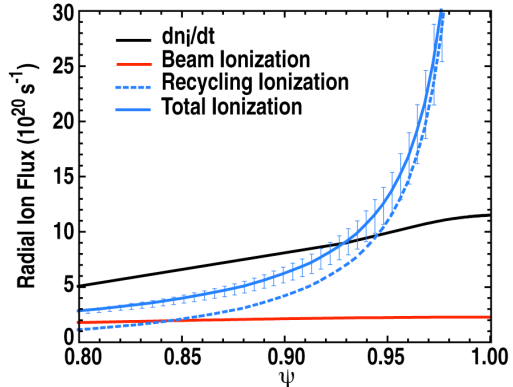


Fig. 6. The radial ion flux due to the time rate of change in density profile ( $dn_i / dt$ ), beam ionization, recycling ionization, and the total ionization (sum of beam and recycling sources).



deposition is more central than the pedestal top. The total ionization is plotted as the sum of these two contributions.

The difference between the total ionization and  $dn_i/dt$  curves represent the profile of radial ion flux. Within the pedestal, from  $\psi = 0.95$  outwards, the ion flux is radially outward driven by the strong ionization source. However near the pedestal top,  $\psi \sim 0.95$  the radial flux becomes very small and then negative inside this region. This implies an inward convection, or density pinch, is required to account for the increase in density in this region.

#### 4. Conclusions

Pedestal fueling through edge recycling has been examined with OEDGE interpretive modeling for high-density discharges in DIII-D. Steady-state conditions were assumed for a comparison between a high plasma current, high-density discharge and a lower current and density discharge. The radial ion flux profiles, inferred from edge recycling and neutral beam ionization, were remarkably similar in the two cases. The greater density pedestal top and gradient at high current indicates a diffusion coefficient scaling with  $1/I_p$  if no inward density pinch is assumed. A future exercise will be to extract the radial profile of the diffusion coefficient and examine its scaling. The decrease in radial flux towards the pedestal top would indicate the diffusion coefficient reaches a minimum near the top of the pedestal. An alternative interpretation would be a more constant diffusion coefficient that includes an inward pinch velocity. Further work with higher pedestal density and time dependent experiment and analysis will be required to discriminate between the two interpretations.

A second analysis has taken into account the time dependence of the pedestal density profile between ELMs. For this time dependent case the modeled ionization source is found to be somewhat less than required to account for the rise in density inward of the top of the pedestal. However, further work is required to produce a convincing case that this density rise is primarily due to inward convection, or a density pinch. First the inboard divertor should be better documented to reduce uncertainty in the neutral source from that region. Secondly the neutral beam heating could be replaced with ECH heating to maintain the H-mode. This would essentially remove all central fueling and any density increase would have to result from plasma transport. If an inward pinch can be shown to be responsible for a significant fraction of the pedestal and core density in H-mode then the central fueling requirements for future large tokamaks such as ITER will be reduced.

#### Acknowledgment

This work was supported by the US Department of Energy under DE-FC02-04ER54698 and DE-AC05-00OR22725.

## References

- [1] A.S. Kukushkin, et al., Nucl. Fusion **49** (2009) 075008.
- [2] A.S. Kukushkin, A.R. Polevoi, H.D. Pacher, et al., J. Nucl. Mater. **415** (2011) s497.
- [3] R.J. Groebner, M.A. Mahdavi, A.W. Leonard, *et al.*, Phys. Plasmas **9** (2002) 2134.
- [4] J.W. Hughes, B. Labombard, J. Terry, *et al.*, Nucl. Fusion **47** (2007) 1057.
- [5] R.J. Groebner, T.H. Osborne, A.W. Leonard, *et al.*, Nucl. Fusion **49** (2009) 045013.
- [6] W.M. Stacey and R.J. Groebner, Phys. Plasmas, **16** (2009) 102504.
- [7] S. Lisgo, P. Borner, C. Boswell, *et al.*, J. Nucl. Mater. **337-339** (2005) 139.
- [8] S. Lisgo, P.C. Stangeby, J.D. Elder, *et al.*, J. Nucl. Mater. **337-339** (2005) 256.
- [9] D. Reiter, The EIRENE code, <http://www.eirene.de>
- [10] A.W. Leonard, M. Groth, G.D. Porter, *et al.*, J. Nucl. Mater. 390-391 (2009) 470.